Kovove Mater. 50 2012 107–113
DOI: 10.4149/km_2012_2_107

Effect of coated B_4C reinforcement on mechanical properties of squeeze cast A356 composites

A. Mazahery, M. O. Shabani*, M. R. Rahimipour, A. A. Tofigh, M. Razavi

Materials and Energy Research Center (MERC), Tehran, Iran

Received 13 May 2011, received in revised form 17 June 2011, accepted 18 August 2011

Abstract

In the present study, attempts were made to coat the B_4C powders with TiB_2 via a sol-gel process, and then squeeze cast A356 matrix composites reinforced with coated B_4C particles were fabricated. X-ray diffraction studies also confirmed the existence of boron carbide and some other reaction products such as TiB_2, AlB_2 and Al_3BC in composite samples. It was observed that the amount of porosity increased with increasing the volume fraction of composites. Tensile behavior and hardness of unreinforced alloy and composites were evaluated. It was noted that the elastic constant, strain-hardening and UTS of the metal matrix composites (MMCs) were higher than those of the un-reinforced Al alloy and increased with increasing of coated B_4C content. The strengthening of particulate reinforced metal-matrix composites is associated with a high dislocation density in the matrix due to the difference in coefficient of thermal expansion between the reinforcement and the matrix.

Key words: MMCs, aluminum, boron carbide, sol-gel processing

1. Introduction

MMCs are attractive in various applications because of their improved properties. A vast range of MMC materials has been conceived and studied in order to combine the desirable attributes of metal and ceramics. The addition of high strength, high modulus refractory particles to a ductile metal matrix produce a material whose mechanical properties are intermediate between the matrix alloy and ceramic reinforcement. Metals have a useful combination of properties such as high strength, ductility and high temperature resistance but sometimes have low stiffness, whereas ceramics are stiff and strong though brittle. In addition to improved physical and mechanical properties, particulate-reinforced composites are generally isotropic and they can be processed through conventional methods used for metals [1, 2].

Matrices based on Ag, Al, Be, Co, Cu, Fe, Mg, Ni and Ti are all commercially produced and used. By far the largest commercial volumes are for aluminum matrix composites (AMCs), which accounts for 69 % of the annual MMC production by mass [3]. This large commercial volume is the result of their excellent physical, mechanical and tribological properties and also because of good combination of thermal conductivity and dimensional stability [4–8].

The conventional reinforcement materials for AMCs are SiC and Al_2O_3. Due to the higher cost of B_4C powder relative to SiC and Al_2O_3, limited research has been conducted on B_4C reinforced MMCs [9]. Monolithic B_4C ceramic is a low-density material that is very hard, strong and stiff. However, densification of monolithic B_4C requires high temperatures and/or application of high pressures [10].

A356-B_4C composites have the potential to combine the high stiffness and hardness of B_4C with the ductility of Al and result in a strong low-density material. These boron carbides react strongly with Al, resulting in a variety of binary and ternary compounds, including Al_3BC, $AlB_{24}C_4$ (commonly designated as AlB_{10}), $Al_8B_4C_7$, $Al_3B_{48}C_2$ (often known as β-AlB_{12}), AlB_2, $AlB_{12}C_2$, $AlB_{48}C_2$, Al_4C_3 and α-AlB_{12} [11].

According to the type of reinforcement, the fabrication techniques can vary considerably. These techniques are squeeze casting, liquid metal infiltration, spray decomposition and powder metallurgy. The

---

*Corresponding author: tel.: +98 912 563 6709; fax: +98 261 620 1888; e-mail address: vahid_ostadshabany@yahoo.com

Table 1. Chemical composition of A356

Element	Al	Si	Fe	Cu	Mg	Mn	Zn	Ti
wt. %	Balance	7.5	0.10	0.001	0.38	0.02	0.02	0.01

squeeze casting offers good microstructural control at relatively low cost. The pressure applied during solidification in the squeeze casting technique results in excellent feeding during solidification shrinkage [12, 13].

Composite mechanical property enhancement is a function of the volume fraction, size, shape, spatial distribution of the reinforcement and is also dependent upon how well the externally applied load is transferred to the reinforcing phase. Stronger adhesion at the particle/matrix interface improves load transfer, increasing the yield strength and stiffness, and delays the onsets of particle/matrix de-cohesion [14].

In the present study, boron carbide (B_4C) powder was chosen as reinforcement because of its higher hardness (2900–3580 $\mathrm{kg\,mm^{-2}}$) than the conventional and routinely used reinforcement such as SiC, Al_2O_3, etc. Further its density (2.52 $\mathrm{g\,cm^{-3}}$) is very close to Al alloy matrix.

Since in Al-B_4C system, the wettability is poor at temperatures near the melting point of aluminum (660 ℃), attention was paid to the fact that B_4C powders coated with some of Ti-compounds might have reasonable wettability with aluminum. Thus, first TiB_2 was coated on the surface of the B_4C particles via sol-gel processing. Then, the A356-coated B_4C composites have been processed using squeeze casting. The results of the mechanical properties of squeeze cast composites are presented here.

2. Experimental procedure

A356 aluminum alloy was employed as the matrix material. The conventional reinforcement materials for A356 are SiC and Al_2O_3. Due to the higher cost of B_4C powder relative to SiC and Al_2O_3, limited research has been conducted on B_4C reinforced MMCs. In this study, the B_4C particles with average particle size of µm were used as the reinforcements. The chemical composition of A356 and B_4C are represented in Tables 1 and 2, respectively. The grain size of B_4C particles was analyzed using a Malvern laser size analyzer.

As a sol-gel precursor, titanium tetraisopropoxide (TTIP) was selected and the precursor was diluted with ethanol. For coating of the titanium oxide, boron carbide powders were dispersed in ethanol, stirred well, and TTIP and distilled water were added to the stirred suspension. The processing was conducted at room temperature at a solution pH of 7.

Table 2. Chemical composition of B_4C

Total boron	77.5 %
Total carbon	21.5 %
Total iron	0.2 %
Total B + C	98 %

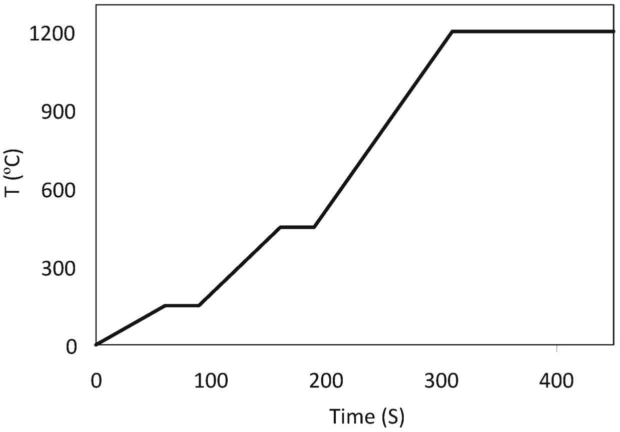

Fig. 1. Heat treatment cycle on B_4C powders after sol-gel process.

Distilled water for hydrolysis was previously diluted by ethanol to inhibit the rapid hydrolysis of TTIP. For sol-gel processing, 0.10 M concentration of TTIP solution was prepared and added to 1 g of B_4C. The amount of water was adjusted to 4 times that of TTIP.

The solution was then aged for 105 min at room temperature, with constant, gentle stirring. After the sol-gel process, the powders were paper-filtered and dried at 140 ℃. When needed, sucrose was introduced in water solution. The powders were heat treated in a graphite crucible and under argon atmosphere. Figure 1 shows the heat treatment cycle that was implemented to eliminate the adsorbed water and to achieve a TiB_2 coating. The powders were analyzed by X-ray diffraction (XRD) and scanning electron microscopy (SEM) which are represented in Figs. 2 and 3, respectively.

For manufacturing of the MMCs, 5, 7.5, 10, 12.5 and 15 vol.% coated B_4C particles were used. The

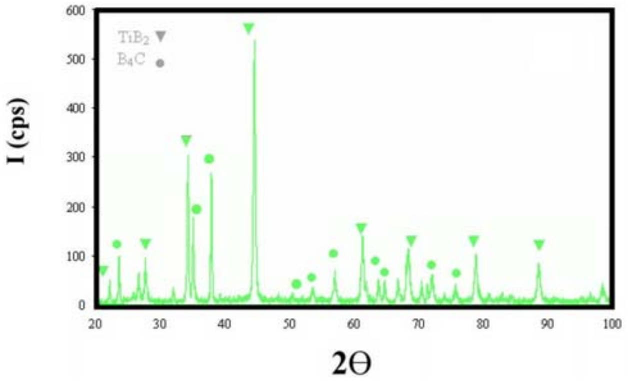

Fig. 2. XRD pattern of the coated B_4C powders.

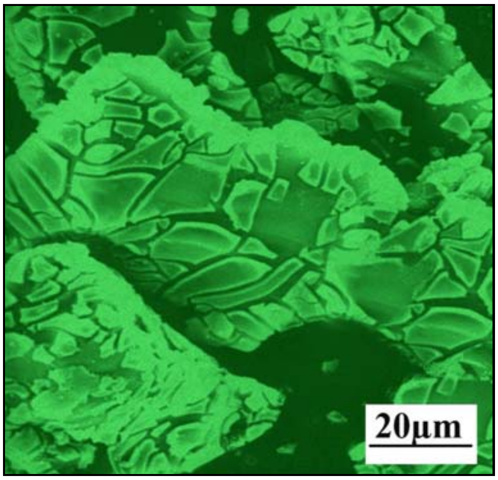

Fig. 3. SEM micrograph of the coated B_4C powders.

melt-particle slurry has been produced by mechanical stirrer. Approximately, 450 g of A356 alloy was charged into the graphite crucible and heated up to a temperature above the alloy's melting point (750 ℃). The temperature control of the electric furnace and molten metal was carried out by an NR911 type thermostat. This thermostat has a special control unit and thermocouples. Thermocouples were inserted into the melt and the furnace to measure their temperature. The graphite stirrer fixed on the mandrel of the drilling machine was introduced into the melt and positioned just below the surface of the melt. Approximately, 1 g reinforcement and aluminum powder mixture were inserted into an aluminum foil by forming a packet. The packets were added into molten metal of crucible when the vortex was formed at every 20 s. The packet of mixture melted and the particles started to distribute around the alloy sample. It was stirred at approximately 600 rev $\min^{-1}$ speed. Argon gas was also blown into the crucible during the operation. The squeeze casting was obtained by pouring composite slurry into preheated permanent die and punch. It is then allowed to solidify under squeeze pressure of 80 MPa for duration of 5 min. High temperature graphite powder was used in the die to facilitate removal of cast blanks from the die after cooling.

The as cast samples were all treated according to T6 condition: solution treated at 540 ℃ for 8 h followed by water-quenching and 155 ℃ artificial aging for 16 h.

For microstructure study, specimens were prepared by grinding through 120, 400, 600, 800 grit papers followed by polishing with 6 µm diamond paste and etched with Keller's reagent (2 ml HF (48 %), 3 ml HCl (conc.), 5 ml HNO_3 (conc.) and 190 ml water). Microscopic examinations of the composites and matrix alloy were carried out using an optical microscope. X-ray diffraction (DebyeScherrer) and energy dispersive X-ray analyses (EDXA) were performed to determine the chemical compositions of the matrix and the reinforcement.

The experimental density of the composites was obtained by the Archimedean method of weighing small pieces cut from the composite cylinder first in air and then in water, while the theoretical density was calculated using the mixture rule according to the weight fraction of the B_4C particles. The porosities of the produced composites were evaluated from the difference between the expected and the observed density of each sample. To study the hardness, the Brinell hardness values of the samples were measured on the polished samples using an indenter ball with 2.5 mm diameter at a load of 31.25 kg. For each sample, 5 hardness readings on randomly selected regions were taken in order to eliminate possible segregation effects and get a representative value of the matrix material hardness. During hardness measurement, precaution was taken to make indentation at a distance of at least twice the diagonal length of the previous indention.

The tensile tests were used to assess the mechanical behavior of the composites and matrix alloy. The composite and matrix alloy rods were machined to tensile specimens according to ASTM.B 557 standard.

3. Results and discussion

Figure 4 shows optical micrograph of the metal matrix composite. Because of the casting process, the B_4C particles were distributed between the dendrite branches and were frequently clustered together, leaving the dendrite branches as particle-free regions in the material. The B_4C particles are pushed by the dendritic fronts and thus it is expected that B_4C particles will be mostly present in the interdendritic region. Because of the movement of the B_4C particles by the dendritic front, there is a tendency of a degree of ag-

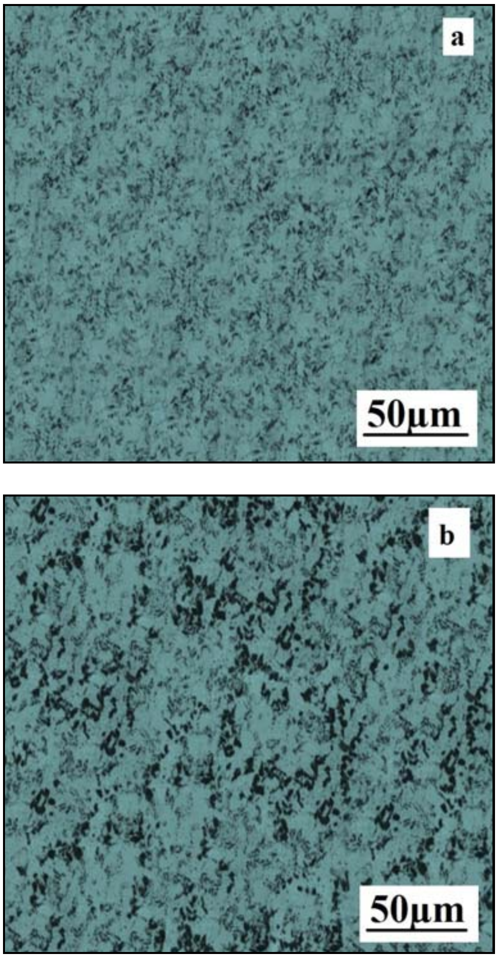

Fig. 4. Typical optical micrographs: (a) the composite with 5 vol.% coated B_4C, (b) the composite with 15 vol.% coated B_4C.

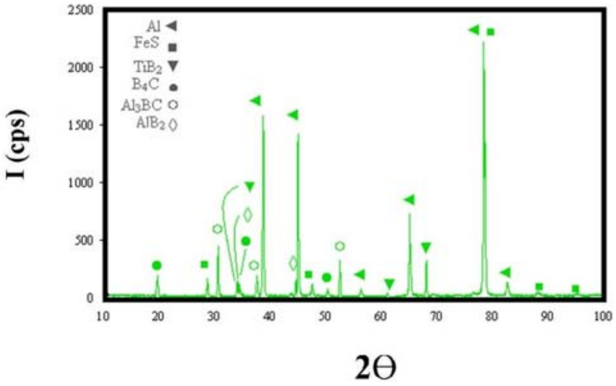

Fig. 5. XRD pattern of the composite produced with 10 vol.% coated B_4C.

glomeration of the particles during casting in composites.

Figure 5 shows the XRD pattern of the composite produced with 10 vol.% B_4C at 750 ℃. It can be seen that B_4C and aluminum are present in the sample. The results for other samples were also similar to this one. In general, the XRD results showed that A356-coated B_4C composites produced under the present processing conditions were composed of various combinations of TiB_2, Al_3BC, AlB_2, and AlB_{12} phases. The type of these phases and their quantity depend on processing conditions. Dissolution of the carbide rapidly saturates the melt with boron and carbon since the maximum solubility of these two elements in aluminum is relatively low (0.1 wt.% and a few tenths of a ppm). Subsequently, AlB_2 nucleates on impurity seeds from the supersaturated melt, while the Al_3BC phase nucleates at the B_4C surface. Growth continues via a classical dissolution-precipitation mechanism [15].

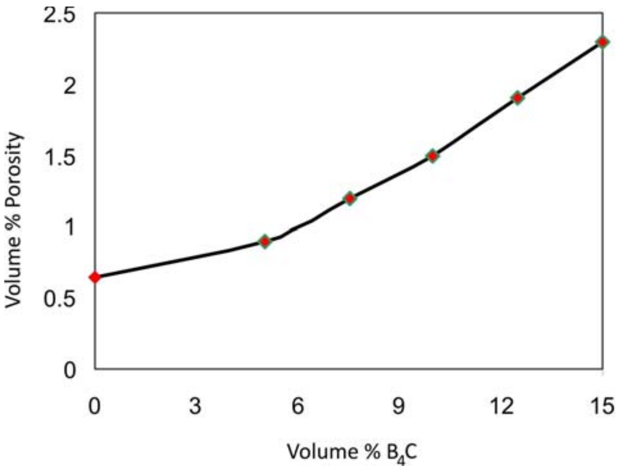

Fig. 6. Variations of porosity of the squeeze cast composites as a function of coated B_4C content.

Figure 6 shows the variation of porosity with the B_4C content. It indicates that increasing amount of porosity is observed with increasing the volume fraction of composites. The porosity level increased, since the contact surface area was increased. It is also reported by the early works [16, 17]. This is attributed to increasing surface gas layers surrounding particles, increasing effective viscosity of suspension resulting in a higher gas hold up as well as improper filling of the gaps between adjacent particles, and increasing sites for heterogeneous pore nucleation [18–20].

The results of hardness tests are shown in Fig. 7. For composite materials containing a soft matrix and a hard reinforcing phase, as in the case of particle reinforced composites, the selection of the region in the sample for evaluating the hardness data is very crucial. In order to obtain the average values of hardness, predominant areas in the soft matrix or the hard reinforcing phase should be avoided so that the average values of hardness are attained from these measurements. The hardness of the MMCs increases with the volume fraction of particulates in the alloy matrix.

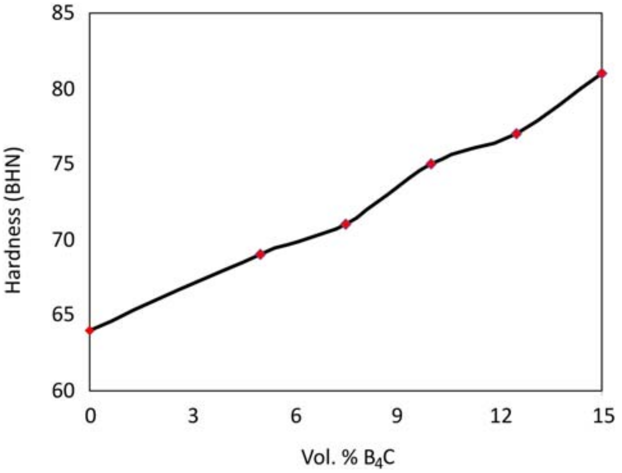

Fig. 7. Variations of hardness value of the samples as a function of coated B_4C content.

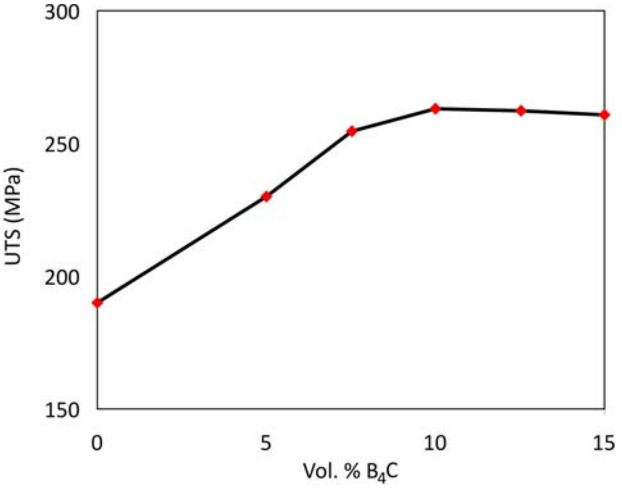

Fig. 8. Variations of UTS value of the samples as a function of vol.% B_4C particulates.

The higher hardness of the composites can be attributed to the fact that B_4C particles act as obstacles to the motion of dislocation [21–25]. As shown, hardness increases with the amount of present B_4C particles. The dispersion of B_4C particles enhances the hardness, as particles are harder than Al alloy, the materials render their inherent property of hardness to the soft matrix.

Figure 8 shows the variations of ultimate tensile stress (UTS) of the composites with the variations of volume fraction. Note that the volume fraction of ceramic particles quoted in this figure is the sum of all three main present ceramic phases: coated B_4C, AlB_2, and Al_3BC. Each value of ultimate tensile strength is an average of at least three tensile specimens. The strength of the composites increases with the increase in reinforcement content. According to the results of this experiment, quite significant improvement in strength is noted when 10 vol.% B_4C particles are added; further increase in B_4C content leads to reduction in strength values.

The great enhancement in values of UTS observed in composites relative to monolithic aluminum is due to grain refinement, the strong multidirectional stress at the A356/B_4C interface, small particle size and low degree of porosity which leads to effective transfer of applied tensile load to the uniformly distributed strong B_4C particulates.

The amount of interface area, nevertheless, increases with increase in B_4C content, and the micro-porosities also increase with increase in B_4C content. On the other hand, increasing dislocation, i.e. defects induced around the B_4C particles due to the differences in the thermal expansion coefficients of Al and B_4C, might result in debonding of the interface and decrease in UTS in the composites with more B_4C volume fraction [17]. Hereby, it is believed that strengthening and weakening factors of mechanical properties could neutralize the effect of each other and thus, the composite containing 10 vol.% B_4C exhibits the maximum ultimate tensile stress.

In case of composites, the plastic flow of matrix is constrained due to the presence of these rigid and very strong B_4C particles. It has been understood that the plastic flow of the composite is due to the plastic flow of the matrix. The strain-hardening of the composite is primarily due to hardening of the matrix during its plastic flow. The strain-hardening of matrix is expected to be influenced by the following factors: (i) dislocation density and dislocation-to-dislocation interaction, (ii) constraint of plastic flow due to resistance offered by B_4C-particles. The dislocation density in the matrix of the composite might be increased with increase in B_4C [26]. To keep the continuity of the composite material under the external load, which requires no formation of any voids and cracks along the particle-matrix interface, a strong internal stress would develop between B_4C particles and the matrix (increased dislocation density). It is expected that due to the thermal mismatch stress ($\mathrm{CTE}_{\mathrm{B4C}} = 5 \times 10^{-6}$), there is a possibility of increased dislocation density within the matrix. The difference between the coefficient of thermal expansion (CTE) values of matrix and ceramic particles generates thermally induced residual stresses and increase dislocations density upon rapid solidification during the fabrication process. This type of internal stress would resist the slip behavior in the metal matrix, and hence, the strain-hardening rate would increase. Similar fact is also true for plastic constraint to the matrix due to particle addition. As seen in Fig. 4, dendrite branches of the Al matrix are surrounded by the B_4C particles and these particles along the dendrite boundaries act as barriers to the slip behavior of the matrix and, hence, strengthen the composite material. This strengthening mechanism is similar to the conventional theory of grain-boundary strengthening in which the grain boundaries block the dislocation movement during plastic deformation. However, this effect of the reinforcing B_4C particles along grain boundaries is obviously much stronger [27, 28].

The above argument should also hold, at least partially, for reasoning the contribution of the reinforcing particles to the increase of the elastic constant in discontinuous reinforcement MMCs, since the load-transfer process is also involved in the elastic range [29, 30].

On the other hand, the microscopic nonuniformity of the particle distribution, created by dendrite structure formation and usually in the form of clustering, is considered as the reason for internal stresses and also stress triaxiality, which are responsible not only for the special hardening behavior, but also for the early appearance of particle cracking, particle interface debonding, and void formation in the matrix [30–32].

4. Conclusion

In this study, B_4C particles were coated with TiB_2 and incorporated into aluminum matrix via squeeze casting. The phases detected by XRD were composed of various combinations of TiB_2, Al_3BC, AlB_2, and AlB_{12}. The B_4C particles were distributed between the dendrite branches and refined the grain structure of the cast materials. Porosity level increased slightly with increasing particulate content. These results can be attributed to the increased surface area of the B_4C particles which can in turn increase the porosity levels. The hardness of the MMCs increases with the volume fraction of particulates in the alloy matrix due to the increasing ceramic phase of the matrix alloy. The higher hardness of the composites could be attributed to the fact that B_4C particles act as obstacles to the motion of dislocation.

It was noted that UTS of the MMCs was higher than that of the un-reinforced Al alloy and increased with increasing of B_4C content.

References

[1] SURESH, S.—MORTENSEN, A.—NEEDLEMAN, A.: Fundamentals of Metal Matrix Composites. Oxford, Butterworth-Heinemann 1993.

[2] DEUIS, R. L.—SUBRAMANIAN, C.—YELLUP, J. M.: Compos. Sci. Technol., *57*, 1997, p. 415. http://dx.doi.org/10.1016/S0266-3538(96)00167-4

[3] RITTNER, M.: Metal Matrix Composites in the 21st Century: Markets and Opportunities. Norwalk, CT, BCC, Inc. 2000.

[4] SHABANI, M. O.—MAZAHERY, A.—BAHMANI, A.—DAVAMI, P.—VARAHRAM, N.: Kovove Mater., *49*, 2011, p. 253.

[5] SHABANI, M. O.—MAZAHERY, A.—RAHIMIPOUR, M. R.—TOFIGH, A. A.—RAZAVI, M.: Kovove Mater., *50*, 2012, p. 25.

[6] MAZAHERY, A.—SHABANI, M. O.: JOM, *64*, 2012, p. 323.

[7] COUTURIOR, R.—DUCRET, D.—MERLE, P.—DISSER, J. P.—JOUBERT, P.: J. Eur. Ceram. Soc., *17*, 1997, p. 1861. http://dx.doi.org/10.1016/S0955-2219(97)87873-9

[8] LIM, S. C.—GUPTA, M.—REN, L.—KWOK, J. K. M.: J. Mater. Process. Technol., *89&90*, 1999, p. 591.

[9] KOUZELI, M.—MORTENSEN, A.: Acta Mater., *50*, 2002, p. 39. http://dx.doi.org/10.1016/S1359-6454(01)00327-5

[10] THEVENOT, F.: J. Eur. Ceram. Soc., *6*, 1990, p. 205. http://dx.doi.org/10.1016/0955-2219(90)90048-K

[11] VIALA, J. C.—BOUIX, J.: J. Mater. Sci., *32*, 1997, p. 4559. http://dx.doi.org/10.1023/A:1018625402103

[12] NAI, S. M. L.—GUPTA, M.: Compos. Struct., *57*, 2002, p. 227. http://dx.doi.org/10.1016/S0263-8223(02)00089-2

[13] HASHIM, J.—LOONEY, L.—HASHMI, M. S. J.: J. Mater. Process. Technol., *92/93*, 1999, p. 1. http://dx.doi.org/10.1016/S0924-0136(99)00118-1

[14] EVANS, A.—MARCHI, C. S.—MORTENSEN, A.: Metal Matrix Composites in Industry: An Introduction and a Survey. Dordrecht, Netherlands, Kluwer Academic Publishers 2003. http://dx.doi.org/10.1007/978-1-4615-0405-4

[15] PYZIK, A. J.—AKSAY, I. A.: Processing and Microstructural Characterization of B4C-AI Cermets. US Patent No: 4702770, 1987.

[16] EL MAHALLAWY, N. A.—TAHA, M. A.—LOFTI ZAMZAM, M.: J. Mat. Process. Tech., *40*, 1994, p. 73. http://dx.doi.org/10.1016/0924-0136(94)90478-2

[17] KOK, M.: Preparation and Some Properties of SiC Particle Reinforced Al Matrix. [Ph.D. Thesis]. The Institute of Science and Technology of Elazig University, Turkey 1999.

[18] ZHOU, W.—XU, Z. M.: J. Mater. Process. Technol., *63*, 1997, p. 358. http://dx.doi.org/10.1016/S0924-0136(96)02647-7

[19] RAY, S.: In: Proceedings of the Survey on Fabrication Methods of Cast Reinforced Metal Composites. Storrs, ASM/TMS 1988, p. 77.

[20] LLOYD, D. J.—CHAMBERLAIN, B.: In: Proceedings of the International Symposium on Advances in Cast Reinforced Metal Composites. Eds.: Fishman, S. G., Dhingra, A. K. Materials Park, ASM International 1988, p. 263.

[21] HOSKING, F. M.—FOLGAR PORTILLO, F.—WUNDERLIN, R.—MEHRABIAN, R.: J. Mater. Sci., *17*, 1982, p. 477. http://dx.doi.org/10.1007/BF00591483

[22] ROY, M.—VENKATARAMAN, B.—BHANUPRASAD, V. V.—MAHAJAN, Y. R.—SUNDARARAJAN, G.: Metall. Trans. A, *23*, 1992, p. 2833. http://dx.doi.org/10.1007/BF02651761

[23] CHUNG, S.—HWANG, B. H.: Tribol. Int., *27*, 1994, p. 307.

http://dx.doi.org/10.1016/0301-679X(94)90024-8

[24] SKOLIANOS, S.—KATTAMIS, T. Z.: Mater. Sci. Eng. A, *163*, 1993, p. 107. http://dx.doi.org/10.1016/0921-5093(93)90584-2

[25] BINDUMADHAVAN, P. N.—WAH, H. K.—PRABHAKAR, O.: Wear, *248*, 2001, p. 112. http://dx.doi.org/10.1016/S0043-1648(00)00546-9

[26] ZHAO, Y. T.—ZHANG, S. L.—CHEN, G.—CHENG, X. N.—WANG, C. Q.: Compos. Sci. Technol., *68*, 2008, p. 1463. http://dx.doi.org/10.1016/j.compscitech.2007.10.036

[27] EJIOFOR, J. U.—REDDY, R. G.: Mat. Sci. Eng. A, *259*, 1999, p. 314. http://dx.doi.org/10.1016/S0921-5093(98)00907-1

[28] YUNG-CHANG KANG—SAMMY LAP-IP CHAN: Mat. Chem. Phys., *85*, 2004, p. 438.

[29] LONG, S.—BEFFORT, O.—CAYRON, C.—BONJOUR, C.: Mat. Sci. Eng. A, *269*, 1999, p. 175. http://dx.doi.org/10.1016/S0921-5093(99)00163-X

[30] CHRISTMAN, T.—NEEDLEMAN, A.—SURESH, S.: Acta Metall., *37*, 1989, p. 3029. http://dx.doi.org/10.1016/0001-6160(89)90339-8

[31] ZHIRUI WANG—TZI-KANG CHEN: Metall. Trans, *24A*, 1993, p. 197.

[32] SURESH, K. R.—NIRANJAN, H. B.—JEBARAJ, P. M.—CHOWDIAH, M. P.: Wear, *255*, 2003, p. 638. http://dx.doi.org/10.1016/S0043-1648(03)00292-8